This is the Pre-Published Version.

This is the peer reviewed version of the following article: Wong, M.T. and Kwok, K.W. (2015), Low-Temperature Sintered K0.5Na0.5NbO3-Based Ceramics for Vibratory Gyro-sensor Applications. Int. J. Appl. Ceram. Technol., 12: E149-E155, which has been published in final form at https://doi.org/10.1111/ijac.12344. This article may be used for non-commercial purposes in accordance with Wiley Terms and Conditions for Use of Self-Archived Versions. This article may not be enhanced, enriched or otherwise transformed into a derivative work, without express permission from Wiley or by statutory rights under applicable legislation. Copyright notices must not be removed, obscured or modified. The article must be linked to Wiley's version of record on Wiley Online Library and any embedding, framing or otherwise making available the article or pages thereof by third parties from platforms, services and websites other than Wiley Online Library must be prohibited."

Low-Temperature Sintered $K_{0.5}Na_{0.5}NbO_3$-Based Ceramics for Vibratory Gyro-sensor Applications

Mau Tak Wong and Kin Wing Kwok*

Department of Applied Physics and Materials Research Centre

The Hong Kong Polytechnic University, Kowloon, Hong Kong, China

For Peer Review

* Corresponding author. Email: apkwkwok@polyu.edu.hk; Tel: +852 27665667; Fax: +852 23337629

Abstract

$0.91K_{0.47}Na_{0.47}Li_{0.06}NbO_3$-$0.09NaSbO_3$ lead-free piezoelectric ceramics were prepared at 1000°C by using a sintering aid comprising of Cu and Ba in a molar ratio of 71.5/28.5. A dense structure with a high density of 4.43 g/cm^3 was obtained for the ceramic added with 2.5 wt% of the sintering aid. Probably due to the smaller grains and doping of Cu^{2+}, the piezoelectric coefficient and dielectric loss were reduced to 120 pC/N and 1.0%, respectively. The ceramics were then fabricated into vibratory gyro-sensors of dimensions 0.6mm×0.6mm×4mm; and good sensitivity (~0.7 mV/dps) was obtained in the range of -360 dps to 360 dps.

For Peer Review

1. INTRODUCTION

Multilayered piezoelectric ceramics have been widely used in various applications, especially in actuator applications such as ultra-small scale motion related applications and control systems for the lenses of cameras and microscopes.[1] The multilayered structure can produce a large electric-field-induced displacement under a relatively low driving voltage. Co-firing with inner electrodes is commonly employed in industries to fabricate multilayered ceramics. Platinum as well as base metal, such as nickel, inner electrodes can be used for co-firing with ceramics at high temperatures up to 1300°C. However, platinum is very expensive and base metal requires a reducing environment for preventing oxidation. Firing in a reducing environment will produce oxygen vacancies and then degrade the properties of most piezoelectric ceramics, including the most widely used lead zirconate titante (PZT) piezoelectric ceramics.[2] A post annealing in an oxidizing atmosphere is hence generally required to re-oxidize the ceramics, which would introduce production cost as well as quality fluctuation.[3] Therefore, it is preferred to lower the sintering temperature of the ceramics so as to co-fire with inexpensive inner electrodes such as Ag/Pd. Liquid phase sintering is a typical and effective method widely used in industries to lower the sintering temperature of ceramics.[4] It generally involves the use of a number of sintering aids that have a low melting temperature or can form a liquid eutectic at low temperatures. Sintering aids such as PbO, Cu_2O, Li_2CO_3 and Bi_2O_3 have been successfully used to lower the sintering temperature of lead-based piezoelectric ceramics below 1000°C.[5-6]

For environmental protection reasons, lead-free piezoelectric ceramics have been extensively studied for replacing the lead-based piezoelectric ceramics in various applications, such as actuators, sensors and transducers. Among various candidates, $K_{0.5}Na_{0.5}NbO_3$ (KNN)-based ceramics are the promising ones because of their relatively high Curie

For Peer Review

temperature and good piezoelectric responses.[7-8] Owing to the low melting temperature (1140°C) and the high volatility of the alkaline elements, it is very difficult to obtain dense and well-sintered KNN ceramic using the conventional sintering process. The poor sinterability of KNN ceramics can be improved by the formation of new solid solutions with other ferroelectrics or non-ferroelectrics, e.g. KNN-$SrTiO_3$ and KNN-$LiSbO_3$,[9-10] and by the use of sintering aids, e.g. MnO_2 and CuO.[11-12] It has been shown that, via the composition modification, the orthorhombic-tetragonal phase transition temperature of some KNN-based ceramics can be adjusted to room temperature, and then leading to significant enhancements in the piezoelectric properties.[9-10] Our recent studies have shown that, owing to the co-existence of the orthorhombic and tetragonal phases, the $0.91K_{0.47}Na_{0.47}Li_{0.06}NbO_3$-$0.09NaSbO_3$ (KNLN-NS) ceramic exhibits a high piezoelectric coefficient d_{33} (305 pC/N) and large electromechanical factors k_p and k_t (0.51).[13] The KNLN-NS ceramic has also been used to fabricate ultrasonic transducers and excellent performance has been obtained. In the present work, the sintering temperature of the KNLN-NS ceramics were lowered from 1080°C to 1000°C by using a CuO-$BaCO_3$ complex additive as a sintering aid, and the effects of the sintering aid on their dielectric and piezoelectric properties were studied. It is anticipated that owing to the low sintering temperature, the ceramics can be co-fired with Ag/Pd (70/30) inner electrodes in fabricating multilayered components. Our previous work has shown that continuous Ag/Pd (70/30) inner electrodes can be obtained via multiple screen-printing and co-firing with $CaBi_4Ti_4O_{15}$-based ceramics at a low sintering temperature of 1000°C.[14] Fabrication of KNLN-NS multilayered ceramics with Ag/Pd (70/30) inner electrodes is planned as a next stage of our research work. The low-temperature sintered ceramics were then fabricated into vibratory gyro-sensors for evaluating their use in practical applications. As both the direct and converse piezoelectric effects were applied in the gyro-sensors, the sensing and actuating capabilities of the ceramics could be evaluated.

For Peer Review

2. PREPARATION AND CHARACTERIZATION OF KNLN-NS-CB CERAMICS

$0.91K_{0.47}Na_{0.47}Li_{0.06}NbO_3$-$0.09NaSbO_3$ ceramics added with x wt% of a CuO-$BaCO_3$ complex additive (abbreviated as KNLN-NS-CB-x) were prepared by a conventional ceramic fabrication technique using analytical-grade carbonate and metal oxide powders: K_2CO_3 (99%), Na_2CO_3 (99%), Li_2CO_3 (99%), Nb_2O_5 (99.99%), Sb_2O_3 (99%), CuO (99%) and $BaCO_3$ (99.5%). The CuO-$BaCO_3$ complex additive in a molar ratio of 71.5/28.5 was used as a sintering aid to lower the sintering temperature. The weight percentage of the additive (i.e. x) used in the present work was 0.0, 1.25, 2.5 and 3.75, respectively. The powders in the stoichiometric ratio of the compositions $0.91K_{0.47}Na_{0.47}Li_{0.06}NbO_3$-$0.09NaSbO_3$ were first mixed thoroughly in ethanol using zirconia balls for 8 h, and then dried and calcined at 800°C for 6 h. After the calcination, a stoichiometric amount of the CuO-$BaCO_3$ sintering aid was added. The resulting mixture was ball-milled again for 8 h and mixed thoroughly with a polyvinyl alcohol binder solution, and then pressed into disk samples with a diameter of 12 mm. The disk samples were finally sintered at 1000°C for 8 h in air. Silver electrodes were fired on the top and bottom surfaces of the samples for the measurements of dielectric and ferroelectric properties.

The crystallite structures of the sintered samples were examined using X-ray diffraction (XRD) analysis with CuK_α radiation (SmartLab, Rigaku Co., Japan). The microstructures were observed using a scanning electron microscope (SEM) (JSM-6490, JEOL Ltd., Japan). The density ρ of the ceramics was measured by the Archimedes method in water. An impedance analyzer (HP 4194A, Agilent Technologies Inc., Palo Alto, CA) was used to measure the dielectric constant ε_r and dielectric loss tan δ. The piezoelectric coefficient d_{33} was measured using a piezo-d_{33} meter (ZJ-3A, China).

For Peer Review

2.1 Density and Microstructures

Fig. 1 shows the observed ρ of the KNLN-NS-CB-x ceramics, while the SEM micrographs of the ceramics with x = 0, 1.25 and 2.5 are shown in Fig. 2. For the KNLN-NS-CB-0 (i.e. KNLN-NS) ceramic, the observed ρ was quite low (~ 4.0 g/cm^3), indicating that it was not well sintered. Obviously, this should be due to the incomplete densification arisen from the low sintering temperature. As shown in Fig. 2a, the ceramic possessed a porous structure and most of the grains were very small (< 0.5 μm). As x (the wt% of the CuO-$BaCO_3$ sintering aid) increased, the observed ρ increased, reaching a high and saturated value of ~4.43 g/cm^3 at x ≥ 2.50 (Fig. 1). As shown in Fig. 2c, the KNLN-NS-CB-2.5 ceramic possessed a dense structure and the grains were much uniform and larger, having a diameter of ~2 μm. Although the grains were smaller than those of the KNLN-NS ceramics sintered at a higher temperature of 1080°C (~4μm),[13] the ceramics were well sintered, suggesting that the CuO-$BaCO_3$ sintering aid was effective in promoting the densification at a low temperature of 1000°C. It should be ascribed to the eutectic mixture of CuO-$BaCO_3$ formed at 890°C, which wets the solid grains and provides a capillary force to pull them together. Because of the solid solubility in the liquid, the mass transport rate is increased, and thus promoting the grain coarsening and densification of the ceramics.[4]

The XRD patterns of the ceramics are shown in Fig. 3. All the ceramics possessed a perovskite structure. A small amount of secondary phase ($K_3LiNb_6O_{17}$) was observed in the KNLN-NS-CB-0 and KNLN-NS-CB-3.75 ceramics, which should probably be arisen from the incomplete sintering or segregation of the alkali elements due to the high addition level of CuO-$BaCO_3$. On the other hand, probably due to the small amounts or diffusion into the lattices, no secondary phase relating to the CuO-$BaCO_3$ sintering aid was observed. As also revealed in Fig. 3, the crystal symmetry of the ceramics remained almost unchanged.

For Peer Review

2.2 Dielectric and Piezoelectric Properties

The variations of ε_r and tan δ with x for the un-poled KNLN-NS-CB-x ceramics are shown in Fig. 4. The measurements were carried out shortly after the electrode deposition at 750°C. Probably due to the smaller grain size (Fig. 2) and doping of Cu^{2+},[12] the observed ε_r and tan δ of the KNLN-NS-CB-x ceramics were generally lower than those of the KNLN-NS ceramics sintered at 1080°C (~1500 and 2.5%).[13] On the other hand, it seemed that the dielectric properties were not affected significantly by the porous microstructures. As shown in Fig. 4, the observed ε_r for ceramics with $x > 0$ varied in the range of 600 to 800, while the variation of tan δ was even smaller: in the range of 1.5 % to 3.2%. However, it had been noted that the dielectric loss of the porous ceramics (i.e., $x < 2.50$) were not stable and would increase with time. The observed ε_r and tan δ of the ceramics after storing in laboratories for a few days are also shown in Fig. 4 for comparison. The observed tan δ for the porous ceramics increased significantly after the storage, while there were no significant changes for the dense ceramics. If the porous ceramics were then heated at 120°C for 24 h, the observed tan δ would decrease to the small values. It is hence suggested that the high tan δ values should be caused by the absorbed moisture during the storage.

Fig. 5 shows the variation of d_{33} with x for the KNLN-NS-CB-x ceramics. In general, current leakage will occur in ceramics with high tan δ (e.g., > 10%), and hence they cannot be poled and then cannot be used in practical applications. For the KNLN-NS-CB-x ceramics with $x < 2.50$, as the moisture was removed during the poling at 150°C, they could be effectively poled under a high electric field of 5.0 kV/mm without severe current leakage or electrical breakdown, and exhibited good piezoelectric properties in spite of the porous structure and high tan δ. Similarly, probably due to the smaller grain size (Fig. 2) and doping of Cu^{2+}, the observed d_{33} of the KNLN-NS-CB-x ceramics were generally lower than those of

For Peer Review

the KNLN-NS ceramics sintered at 1080°C (305 pC/N).[13] Nevertheless, as shown in Fig. 5, the observed d_{33} of the low-temperature sintered ceramics increased after the usage of the CuO-$BaCO_3$ sintering aid, and then decreased with increasing x. It was noted that the ceramic with x = 1.25 exhibited the highest d_{33} (153 pC/N) in spite of the incomplete densification (low density and high tan δ). The decrease in d_{33} for the ceramic with x > 2.5 should be partly due to the excess doping of Cu^{2+} and Ba^{2+}. The observed d_{33} of the ceramics after storing in laboratories at room temperature for 2 days are also shown in Fig. 5 for comparison. Although the dielectric loss of the porous ceramics was sensitive to moisture, their piezoelectric properties were stable and were not degraded significantly.

The variations of ε_r and tan δ with x for the poled KNLN-NS-CB-x ceramics are shown in Fig. 6, in which both the data measured shortly after and 2 days after the poling are presented. The observed ε_r and tan δ of the poled ceramics were similar to those of the un-poled samples. For the well-sintered ceramics (i.e., $x \geq 2.5$), both ε_r and tan δ did not change significantly with time. As expected, the observed tan δ of the porous ceramics ($x < 2.50$) increased after the storage, and the increase for the ceramic with x = 0 was larger than that for the ceramic with x = 1.25. However, the changes were not as large as those for the un-poled counter-parts (Fig. 4). These suggest that the poling process (the alignment of dipoles) as well as the doping of Cu^{2+} and Ba^{2+} may limit the moisture absorption and then reduce the changes of tan δ. Similarly, if the poled porous ceramics were heated at 120°C for 24 h, the observed tan δ would decrease to the low values.

Although the piezoelectric properties are not as high as those of the commercially available lead-based ceramics, such as PZT401 from Morgan Electro Ceramics (d_{33} = 315 pC/N), the KNLN-NS-CB-2.5 ceramic should have great potential for practical applications, especially for multilayered components, owing to the lead-free composition and low sintering temperature. Moreover, because of the low dielectric constant (660) and dielectric loss

For Peer Review

(1.3%), it is a good candidate for piezoelectric sensor applications, for which the performance is governed by the piezoelectric voltage coefficients, e.g., $g_{33} = d_{33}/\varepsilon_r\varepsilon_o$ (ε_o is the permittivity of vacuum).[15,16] Similarly, as the KNLN-NS-CB-1.25 ceramics could be poled and exhibited good and stable piezoelectric properties in spite of the moisture sensitive dielectric properties, it should also have great potential for practical applications and was hence fabricated into vibratory gyro-sensors for evaluation as discussed in the following section.

3. FABRICATION AND CHARACTERIZATION OF KNLN-NS-CB VIBRATORY GYRO-SENSORS

The schematic diagram of the piezoelectric vibratory gyro-sensor fabricated using the low-temperature sintered KNLN-NS-CB-1.25 and KNLN-NS-CB-2.5 ceramics is shown in Fig. 7. The sensor was comprised of a stack of two ceramic plates that were poled in opposite directions.[17] The thickness and width of the two ceramic plates were 0.3 mm and 0.6 mm, respectively. They were glued tightly together using conductive epoxy. Two electrodes of the same dimension were deposited on the top surface of the top ceramic plate, while the bottom surface of the bottom ceramic plate was covered with a single electrode. The stack was then mounted on a holder, forming a cantilever as the vibrating part of the gyro-sensor. The length of the gyro-sensor, i.e., the protruded part, was about 4 mm. An impedance analyzer (HP 4194A, Agilent Technologies Inc., Palo Alto, CA) was used to measure the resonance characteristics of the gyro-sensors. A single-axis rate table (1270VS, Ideal Aerosmith) was used to rotate the gyros-sensors at a precise and stable speed ranging from 0 to ±360 °/s (or dps) in evaluating its sensitivity.

3.1 Working principle of the gyro-sensors

For Peer Review

Under an ac voltage across the thickness direction, the bottom ceramic plate extends and shortens along the length direction as a result of the converse piezoelectric effect and Poisson effect (Fig. 8). As the top ceramic plate does not deform by the ac voltage, the stack acts as a bimorph to bend upwards and downwards. Charges are then generated on the two top-electrodes during the bending vibration by the direct piezoelectric effect. Owing to the geometrical symmetry, the currents collected from the two top-electrodes are of the same amplitude and in phase. In gyro-sensor applications, the stack is driven electrically to vibrate at its resonance frequency. When the gyro-sensor is rotated about its length direction, a Coriolis force is induced, exciting the stack to vibrate along its width direction and hence producing different deformations in the ceramic plate. For example, while the thickness of the left part of the ceramic plate is decreased, that of the right part is increased. As a result, the currents collected from the two top-electrodes become different, and the difference is apparently proportional to the induced vibration and then to the rotation speed. As the stack has a square cross-section, the induced vibration occurs at the resonance frequency, and hence the vibration amplitude and the detected currents reach the optimum values.

An electronic readout circuit was developed in this work to analyze the currents and to output a dc voltage that was proportional to the rotation speed (Fig. 8). A charge amplifier was first used to convert the current collected from each top-electrode to a voltage signal. The small difference between the two voltage signals was detected using a differential amplifier. Then, the detected signal that was varying with time at the same frequency of the vibration was demodulated synchronously by a demodulator using the driving voltage as a reference. Finally, a low-pass filter was used to remove the higher order components of the signal from the demodulator, producing a dc voltage proportional to the rotation speed as an output signal.

3.2 Performances of the gyro-sensors

For Peer Review

Fig. 9 shows the resonance characteristics of the gyro-sensors fabricated using the KNLN-NS-CB-1.25 and KNLN-NS-CB-2.5 ceramics. To simulate the actual applications, an ac voltage was applied to the bottom plate of the gyro-sensors in the measurements to induce the bending vibration of the bimorph (Fig. 8). As the length-to-width ratio of the gyro-sensors was relatively small (~7), the observed resonance peaks were not strong. As shown in Fig. 9a, in spite of the high dielectric loss (19% at 1 kHz), the KNLN-NS-CB-1.25 ceramic gyro-sensor exhibited a weak resonance at ~23 kHz. Probably due to the denser structure, the KNLN-NS-CB-2.5 ceramic gyro-sensor exhibited the resonance at a higher frequency (~33 kHz). This may also be partly due to the deviation in the length of the vibrating part. As the gyro-sensor was glued on a holder using epoxy, the clamping might not be as tight as a fixed end (i.e., the ideal condition for a cantilever). As a result, the actual vibrating part might become longer than the length of the gyro-sensor (i.e., the protruded part) and the resonance frequency might then be lower. Apparently, the resulting deviation became more significant for a short gyro-sensor (e.g., the gyro-sensors with a length of 4 mm fabricated in this work).

Although the piezoelectric properties of the KNLN-NS-CB-x ceramics were not excellent, both the gyro-sensors outputted a steady dc voltage at any rotation speed in the range studied. This also clearly showed that the high dielectric loss arisen from moisture absorption would not affect the performance of ceramics at high frequencies. Fig. 10 shows the variations of the dc output voltage with the rotation speed for the gyro-sensors driven by an ac voltage of 5 V at their resonance frequencies. A linear relationship was obtained for both the gyro-sensors. From the slope of the curves, the sensitivities of the KNLN-NS-CB-1.25 and KNLN-NS-CB-2.5 gyro-sensors were determined as 0.8 mV/dps and 0.6 mV/dps, respectively. The higher sensitivity of the KNLN-NS-CB-1.25 gyro-sensors may also be due to the longer vibrating beam as revealed from its lower resonance frequency. A longer vibrating beam can generate a larger amplitude; and it can also be displaced more and easier

For Peer Review

by the induced Coriolis force. On the basis of the good performance as well as the small size, the low-temperature sintered KNLN-NS-CB-x ceramics should be promising for practical applications, especially for multilayered devices such as miniaturized piezoelectric vibratory gyro-sensors.

4. Conclusion

Lead-free KNLN-NS-CB piezoelectric ceramics were prepared at 1000°C by using a sintering aid comprising of Cu and Ba in a molar ratio of 71.5/28.5. The sintering aid was effective in decreasing the sintering temperature, improving the densification and reducing the dielectric loss. For the ceramic added with 2.5 wt% of the sintering aid, the density was increased to 4.43 g/cm^3 and the dielectric loss was reduced to 1.3 %. However, probably due to the smaller grain size and doping of Cu^{2+}, the piezoelectric coefficient was decreased to 120 pC/N. Although the ceramics added with less sintering aid had a porous structure and their dielectric loss became sensitive to moisture, they could be effectively poled at high temperatures and exhibited relatively good and stable piezoelectric properties. Our results had shown that both the gyro-sensors fabricated using the dense and porous ceramics could output a steady dc voltage in response to rotation, giving a relatively high sensitivity of ~0.7 mV/dps in the range of rotation speed from -360 dps to 360 dps. On the basis of the good piezoelectric properties and performances in gyro-sensors, the low-temperature sintered KNLN-NS-CB piezoelectric ceramics are promising for practical applications, in particular for multilayered components such as miniaturized piezoelectric vibratory gyro-sensors.

Acknowledgements

This work was supported by the Research Grants Council of the Hong Kong Special Administrative Region (Project No. PolyU 5170/13E), the Research Committee (A/C code 1-

For Peer Review

ZV6Y) and the Centre for Smart Materials of The Hong Kong Polytechnic University. The authors would like to thank Mr. Wong Hon Kit and Mr. Wong Wing Fai for their help in characterizing the gyro-sensors.

For Peer Review

REFERENCES

1. Piezoelectric Actuators and Motors - Global Markets and Market Trends, by Innovative Research and Products, Inc. (Stamford, CT, USA www.innoresearch.net).
2. H. Kishi, Y. Mizuno, and H. Chazono, "Base-metal electrode-multilayer ceramic capacitors: Past, present and future perspectives," Jpn. J. Appl. Phy. 42 1-15 (2003).
3. S. Kawada, M. Kimura, Y. Higuchi, and H. Takagi, "(K,Na)NbO_3-based multilayer piezoelectric ceramics with nickel inner electrodes," Appl. Phy. Express 2 111401 (2009).
4. R.M. German, P. Suri, and S.J. Park, "Review: liquid phase sintering," J. Mater. Sci. 44 1-39 (2009).
5. D.L. Corker, R.W. Whatmore, E. Ringgaard, and W.W. Wolny, "Liquid-phase sintering of PZT ceramics," J. Eur. Ceram. Soc. 20 2039-2045 (2000).
6. K.H. Chung, J.H. Yoo, C.B. Lee, D.C. Lee, Y.H. Jeong, and H.G. Lee, "Microstructural, dielectric and piezoelectric properties of low-temperature sintering $Pb(Co_{1/2}W_{1/2})O_3$-$Pb(Mn_{1/2}Nb_{2/3})O_3$-$Pb(Zr,Ti)O_3$ ceramics with the addition of Li_2CO_3 and Bi_2O_3," Sens. Actuators A 125 340-345 (2006).
7. M.D. Maeder, D. Damjanovic, and N. Setter, "Lead free piezoelectric materials," J. Electroceram. 13 385-392 (2004).
8. Y. Saito, H. Takao, T. Tani, T. Nonoyama, K. Takatori, T. Homma, T. Nagaya, and M. Nakamura, "Lead-free piezoceramics," Nature 432 84-87 (2004).
9. R. Wang, R. Xie, K. Hanada, K. Matsusak, H. Bando, and M. Itoh, "Phase diagram and enhanced piezoelectricity in the strontium titanate doped potassium–sodium niobate solid solution," Phys. Stat. Sol. A 202 R57–59 (2005).

For Peer Review

10. D. Lin, K.W. Kwok, K.H. Lam, and H.L.W. Chan, "Structure and electrical properties of $Na_{0.5}K_{0.5}NbO_3$-$LiSbO_3$ lead-free piezoelectric ceramics," J. Appl. Phys. 101 074111 (2007).

11. D. Lin, K.W. Kwok, H. Tian, and H.L.W. Chan, "Phase Transitions and electrical properties of $(Na_{1-x}K_x)(Nb_{1-y}Sb_y)O_3$ lead-free piezoelectric ceramics with MnO_2 sintering aid," J. Am. Ceram. Soc. 90 1458-1462 (2007).

12. D. Lin, K.W. Kwok, and H.L.W. Chan, "Piezoelectric and ferroelectric properties of Cu-doped $K_{0.5}Na_{0.5}NbO_3$ lead-free ceramics," J. Phys. D: Appl. Phys. 41 045401 (2008).

13. D. Lin, and K.W. Kwok, "Piezoelectric properties of $K_{0.47}Na_{0.47}Li_{0.06}NbO_3$-$NaSbO_3$ lead-free ceramics for transducer applications," Int. J. Appl. Ceram. Technol. 8 684-690 (2011).

14. H. Y. Wong, "Development of lead-free piezoelectric ceramic resonators for high-frequency oscillator applications," The Hong Kong Polytechnic University The Department of Applied Physics, Thesis 2008.

15. A. Megriche, L. Lebrun and M. Troccaz, "Materials of $Bi_4Ti_3O_{12}$ type for high temperature acoustic piezo-sensors," Sens. Actuators A 78 88-91 (1999).

16. K.W. Kwok and H.Y. Wong, "Piezoelectric and pyroelectric properties of Cu-doped $CaBi_4Ti_4O_{15}$ lead-free ferroelectric ceramics," J. Phys. D: Appl. Phys. 42 095419 (2009).

17. A. Mori, Vibrating Gyroscope, US Patent 6477897 B1 (2002).

For Peer Review

FIGURE CAPTIONS

Fig. 1 Variation of the density ρ with x for the KNLN-NS-CB-x ceramics

Fig. 2 SEM micrographs of the KNLN-NS-CB-x ceramics: (a) x = 0; (b) x = 1.25; and (c) x = 2.5.

Fig. 3 XRD patterns of the KNLN-NS-CB-x ceramics

Fig. 4 Variations of the dielectric constant ε_r and dielectric loss tan δ with x for the un-poled KNLN-NS-CB-x ceramics. The solid symbols denote the data measured shortly after the electrode deposition at 750°C, while the open symbols denote the data measured after storing in laboratories for 2 days.

Fig. 5 Variations of the piezoelectric coefficient d_{33} with x for the KNLN-NS-CB-x ceramics. The solid and open symbols denote the data measured shortly after and 2 days after the poling, respectively.

Fig. 6 Variations of the dielectric constant ε_r and dielectric loss tan δ with x for the poled KNLN-NS-CB-x ceramics. The solid and open symbols denote the data measured shortly after and 2 days after the poling, respectively.

Fig. 7 Schematic diagram of the piezoelectric vibratory gyro-sensors fabricated using the low-temperature sintered KNLN-NS-CB-1.25 and KNLN-NS-CB-2.5 ceramics.

Fig. 8 Schematic diagram of the characterization set-up for the gyro-sensors.

Fig. 9 Resonance characteristics of the gyro-sensors fabricated using the KNLN-NS-CB-x ceramics: (a) x = 1.25; and (b) x = 2.50.

Fig. 10 Variations of the dc output voltage with the rotation speed for the gyro-sensors fabricated using the KNLN-NS-CB-x ceramics.

For Peer Review

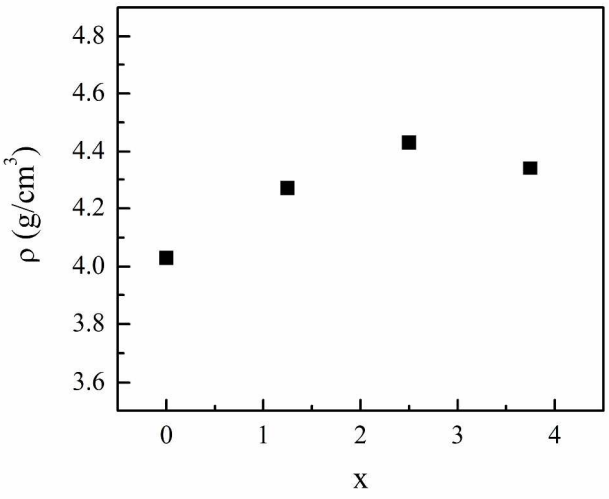

Figure 1 Variation of the density ρ with x for the KNLN-NS-CB-x ceramics.
297x420mm (300 x 300 DPI)

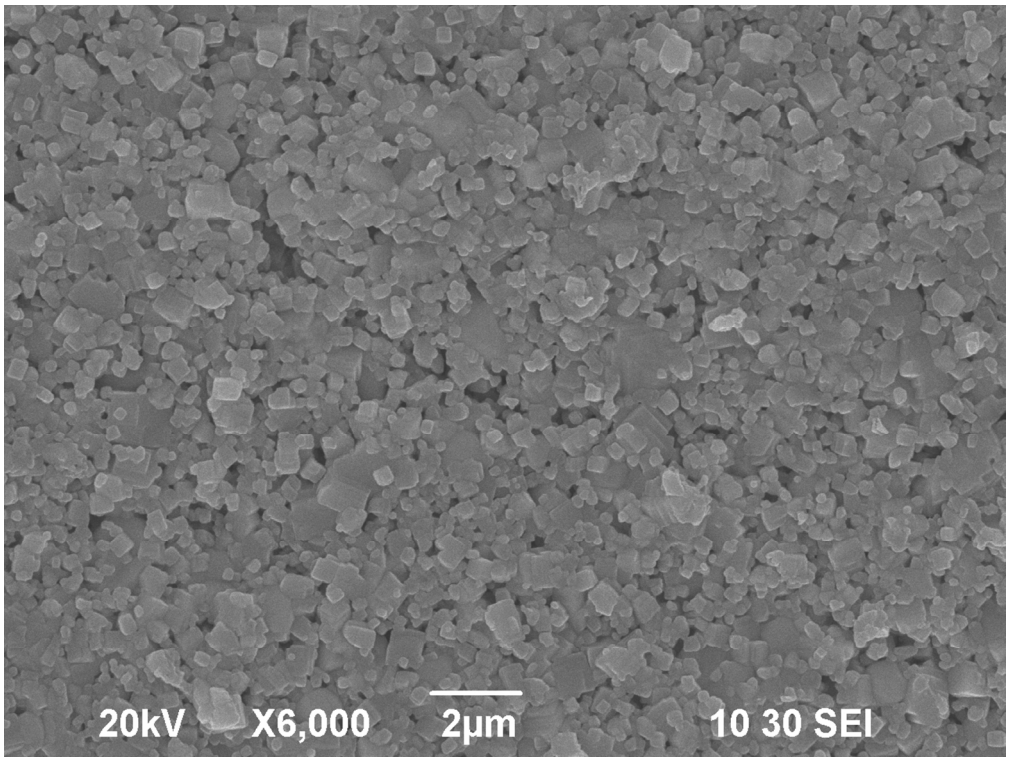

Figure 2a SEM micrographs of the KNLN-NS-CB-x ceramics: x = 0
127x96mm (254 x 254 DPI)

For Review

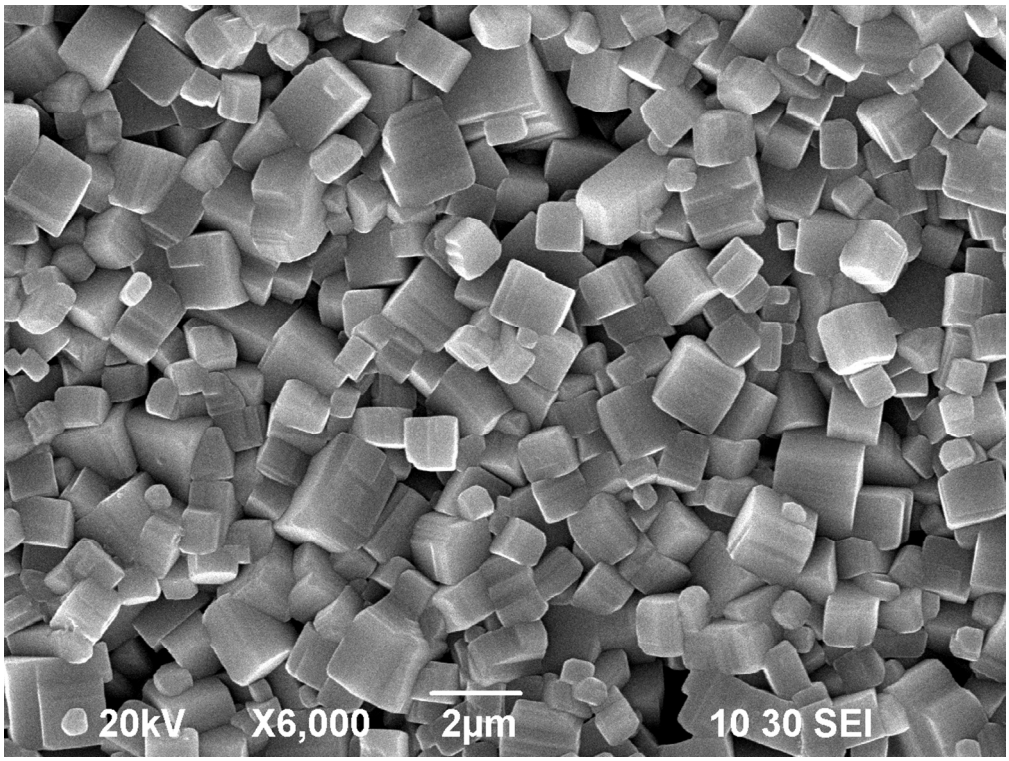

Figure 2b SEM micrographs of the KNLN-NS-CB-x ceramics: x = 1.25
127x96mm (254 x 254 DPI)

Review

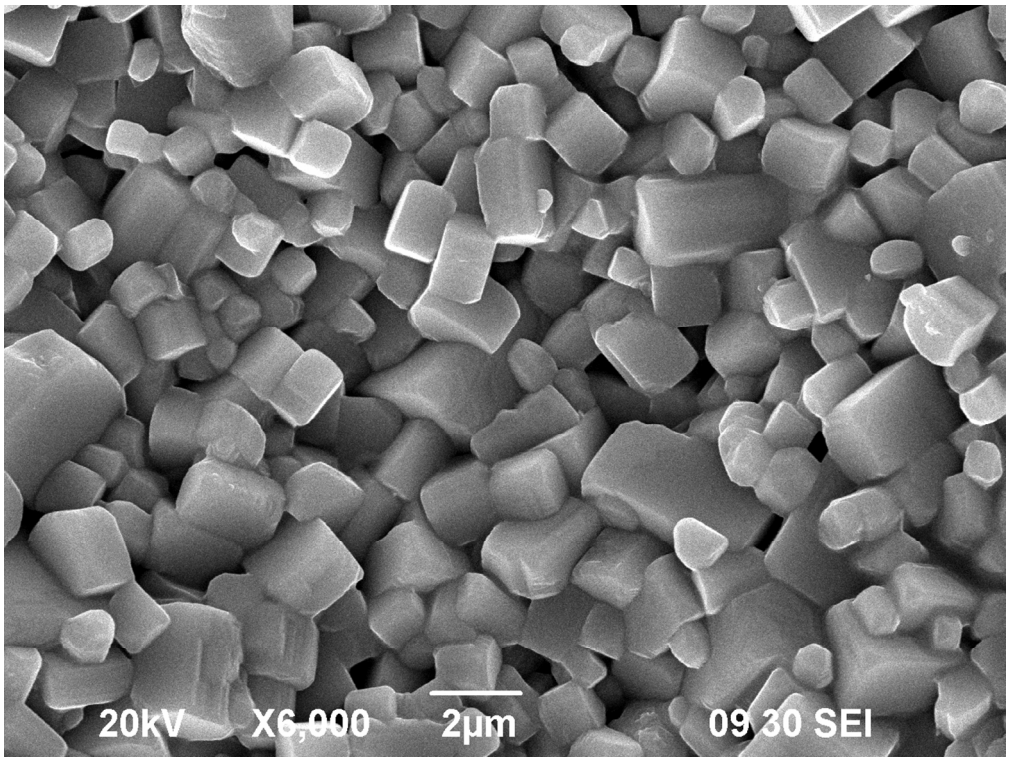

Figure 2c SEM micrographs of the KNLN-NS-CB-x ceramics: x = 2.5
127x96mm (254 x 254 DPI)

For Review

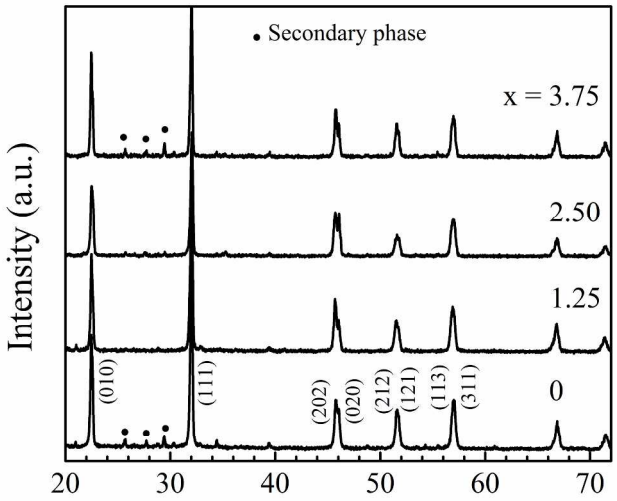

Fig. 3 XRD patterns of the KNLN-NS-CB-x ceramics.
264x333mm (300 x 300 DPI)

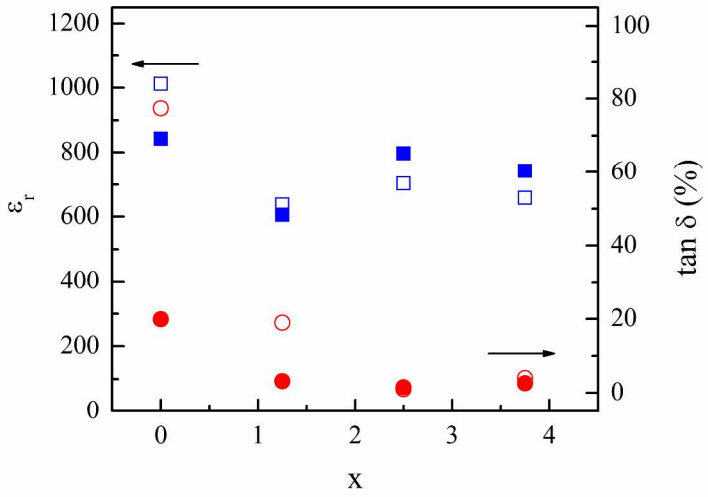

Figure 4 Variations of the dielectric cεonstant ε_r and dielectric loss tan δ with x for the un-poled KNLN-NS-CB-x ceramics. The solid symbols denote the data measured shortly after the electrode deposition at 750°C, while the open symbols denote the data measured after storing in laboratories for 2 days.
297x420mm (300 x 300 DPI)

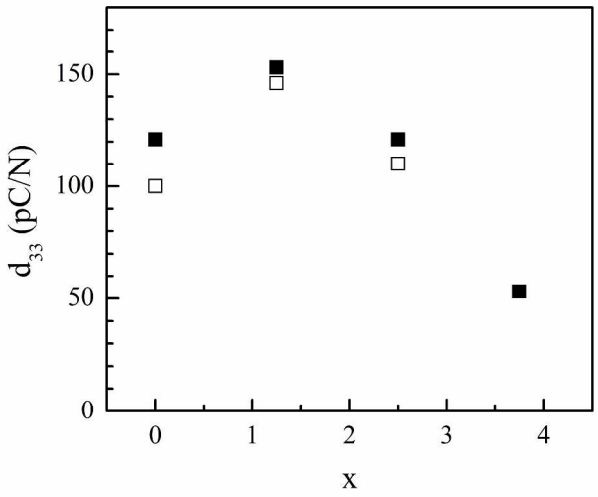

Figure 5 Variations of the piezoelectric coefficient d_{33} with x for the KNLN-NS-CB-x ceramics. The solid and open symbols denote the data measured shortly after and 2 days after the poling, respectively.
297x420mm (300 x 300 DPI)

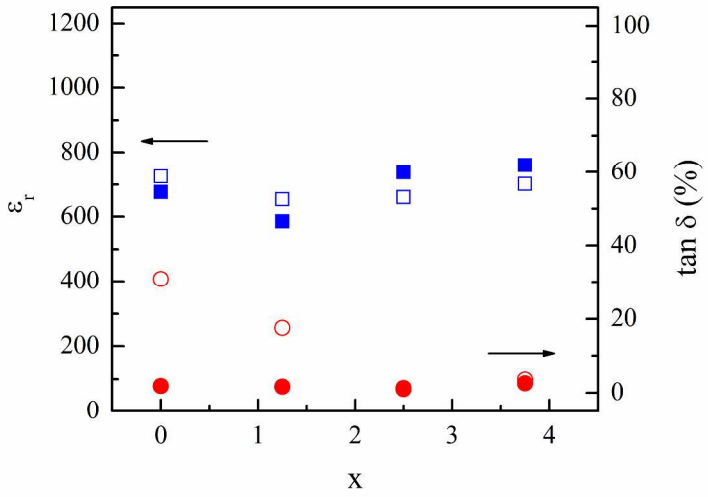

Figure 6 Variations of the dielectric constant ε_r and dielectric loss tan δ with x for the poled KNLN-NS-CB-x ceramics. The solid and open symbols denote the data measured shortly after and 2 days after the poling, respectively.
297x420mm (300 x 300 DPI)

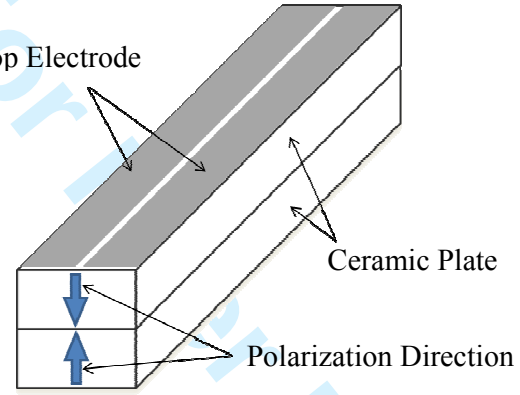

For Peer Review

Fig. 7 Schematic diagram of the piezoelectric vibratory gyro-sensors fabricated using the low-temperature sintered KNLN-NS-CB-1.25 and KNLN-NS-CB-2.5 ceramics.

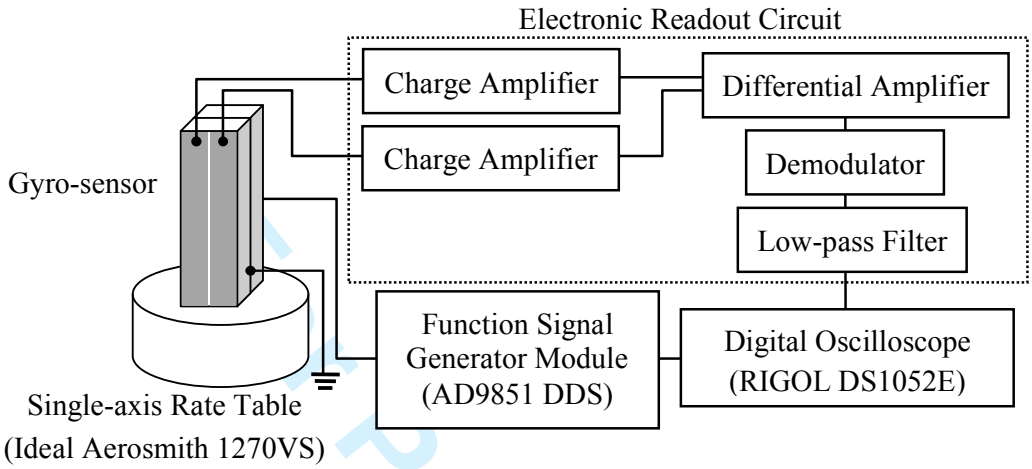

Fig. 8 Schematic diagram of the characterization set-up for the gyro-sensors.

For Peer Review

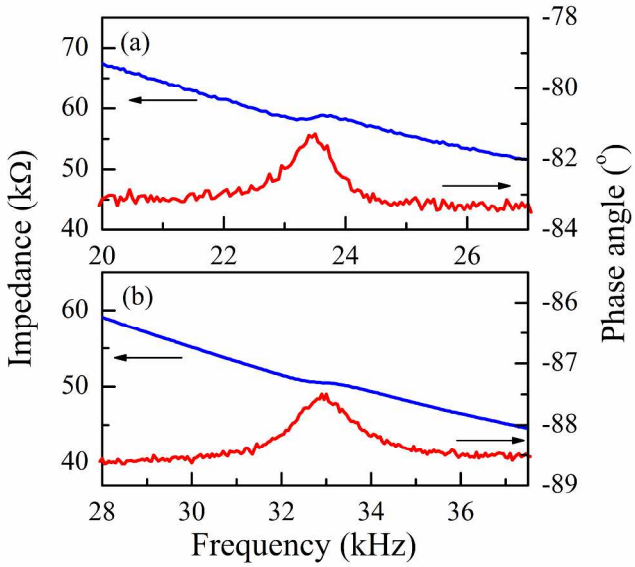

Figure 9 Resonance characteristics of the gyro-sensors fabricated using the KNLN-NS-CB-x ceramics: (a) x = 1.25; and (b) x = 2.50.
281x390mm (300 x 300 DPI)

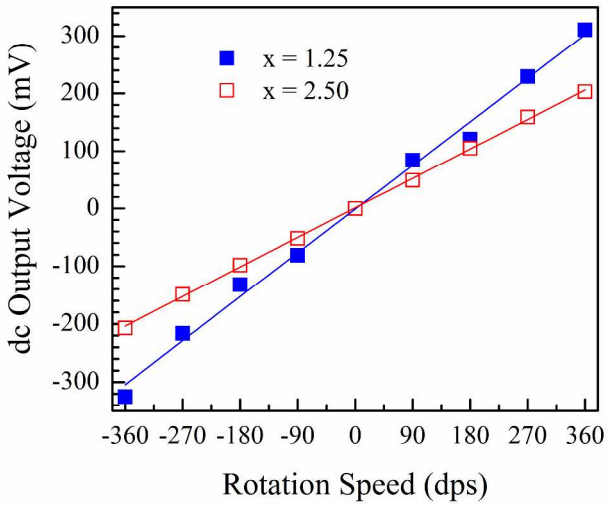

Fig. 10 Variations of the dc output voltage with the rotation speed for the gyro-sensors fabricated using the KNLN-NS-CB-x ceramics.
297x420mm (300 x 300 DPI)